Journal of Fluorescence, Vol. 12, No. 1, March 2002 (© 2002)

Time-Resolved Fluorescence Spectroscopy Study on the Photophysical Behavior of Quantum Dots

W. G. J. H. M. van Sark,[1,4] P. L. T. M. Frederix,[1,2] D. J. van den Heuvel,[1] A. A. Bol,[3] J. N. J. van Lingen,[3] C. de Mello Donegá,[3] H. C. Gerritsen,[1] and A. Meijerink[3]

Received September 27, 2001; accepted December 13, 2001

Room-temperature time-resolved luminescence measurements on *single* CdSe/ZnS quantum dots (QDs) are presented. Fluorescence emission spectra were recorded over periods of up to 30 minutes with a time resolution as small as 6 ms. For QDs in ambient air, a clear 30–40 nm blue shift in the emission wavelength is observed, before the luminescence stops after about 2–3 minutes because of photobleaching. In a nitrogen atmosphere, the blue shift is absent while photobleaching occurs after much longer times (i.e., 10–15 minutes). These observations are explained by photoinduced oxidation. The CdSe surface is oxidized during illumination in the presence of oxygen. This effectively results in shrinkage of the CdSe core diameter by almost 1 nm and consequently in a blue shift. The faster fading of the luminescence in air suggests that photoinduced oxidation results in the formation of non-radiative recombination centers at the CdSe/$CdSeO_x$ interface. In a nitrogen atmosphere, photoinduced oxidation is prevented by the absence of oxygen. Additionally, a higher initial light output for CdSe/ZnS QDs in air is observed. This can be explained by a fast reduction of the lifetime of the long-lived defect states of CdSe QDs by oxygen.

KEY WORDS: Time-resolved fluorescence spectroscopy; quantum dots; CdSe, photoinduced oxidation; fluorescence intermittency.

INTRODUCTION

The unique properties of nanometer-size semiconductor quantum dots (QDs) are responsible for the large (and still increasing) interest that they have received over the past decade [1–4]. The change in the electronic structure as a function of particle size is evident from the variation of emission wavelength [2,5–7]. Because of the confinement of electrons and holes in the nanocrystallites, the energy level scheme resembles that of an atom, with many discrete energy levels. The separation between energy levels increases as the particle size decreases. Since the measurement of *single* QD emission spectra by Blanton *et al.* [8] and Nirmal *et al.* [9], the study of the luminescence of single semiconductor QDs has revealed many interesting properties that cannot be observed for an ensemble of many QDs. Phenomena of fundamental interest such as spectral diffusion and blinking (on/off behavior) are also important for potential applications of single QDs as luminescent labels in biological systems [10–13]. Most studies on spectral diffusion have been performed at cryogenic temperatures. Random spectral diffusion at low temperatures has been related to blinking and therefore ionization of QDs by Auger processes [9,14–17]. As a result of the ionization and subsequent

[1] Department of Molecular Biophysics, Debye Institute, Utrecht University, P.O. Box 80000, 3508 TA Utrecht, The Netherlands
[2] Department of Medical Physiology, Faculty of Medicine, Utrecht University, P.O. Box 80030, 3508 TA Utrecht, The Netherlands.
[3] Department of Physics and Chemistry of Condensed Matter, Debye Institute, Utrecht University, P.O. Box 80000, 3508 TA Utrecht, The Netherlands.
[4] To whom correspondence should be addressed. Tel: +31 30 253 2825. Email: W.G.J.H.M.vanSark@phys.uu.nl

1053-0509/02/0300-0069/0 © 2002 Plenum Publishing Corporation

recombination processes, the charge distribution around the dot changes, resulting in a spectral (Stark) shift of the emission [17,18]. A clear relation between blinking (explained by photoionization) and the occurrence of a spectral jump has been established.

At room temperature, less information is available on spectral diffusion of single QD luminescence. A blue shift of about 10–15 nm has been reported [9,19,20], which was attributed to photooxidation of the QD. This room-temperature blue shift is not random. Here, we further report on the time evolution of the room-temperature emission spectra of single CdSe/ZnS QD over periods up to 30 minutes with a time resolution down to 6 ms. We present results on spectral diffusion (blueing), the disappearance of the emission (bleaching), and on/off behavior (blinking) for two types of CdSe/ZnS QDs (being different in the thickness of the ZnS shell) in two types of atmospheres (air and nitrogen).

EXPERIMENTAL

The ZnS-capped CdSe nanoparticles were synthesized by using a TOP/TOPO method similar to the one described by Hines and Guyot-Sionnest [21–23]. Two batches of overcoated dots were synthesized. For batch 1, about four monolayers of ZnS were grown over the CdSe core, and for batch 2 the thickness amounted to about seven monolayers. The number of monolayers is based on the amounts of precursors used in the synthesis.

The synthesis was performed in a glovebox filled with nitrogen. Stock solutions of Cd, Zn, S, and Se in TOP were prepared. For the Cd/TOP stock solution, 1.6 g (0.011 mol) dimethylcadmium was dissolved in 15.5 ml TOP. The Zn/TOP stock solution was prepared by dissolution of 1.23 g (0.01 mol) diethylzinc in 9.0 ml TOP. Se, 1.3 g (0.016 mol), was dissolved in 16.0 ml TOP, and 2.0 ml (0.01 mol) $(TMS)_2S$ was dissolved in 8.0 ml TOP to obtain the Se/TOP and S/TOP stock solutions, respectively. Cd/Se/TOP and Zn/S/TOP stock solutions were freshly prepared for every synthesis. The Cd/Se/TOP stock solution was prepared by diluting 0.4 ml Cd/TOP and 0.4 ml Se/TOP in 2.0 ml TOP. Dissolution of 1.6 ml S/TOP and 1.12 ml Zn/TOP in 8.28 ml TOP gave the Zn/S/TOP stock solution.

The synthesis was performed by the following method. TOPO, 25 g, was heated to 300°C and kept at this temperature for half an hour to degas and dry the TOPO. The temperature was raised to 370°C. The heater was then removed and the temperature dropped. At 360°C, 1.4 ml Cd/Se/TOP stock solution (containing 0.13 mmol Cd and 0.20 mmol Se) was injected rapidly. The reaction mixture was allowed to cool to 300°C, and at this temperature 5.5 ml of the Zn/S/TOP stock solution (0.62 mmol Zn, 0.88 mmol S) was added in five portions at approximately 20-sec intervals (batch 1). For batch 2, 13.73 ml of the Zn/S/TOP was added in five portions. After this injection the reaction mixture was allowed to cool down to 100°C and was kept at this temperature for 1 hour.

The nanocrystals were purified by precipitation with anhydrous methanol. The precipitate was collected by centrifuging (4,000 rpm, 5 minutes). The precipitate was then washed three times with anhydrous methanol. The nanocrystals were dispersed in doubly distilled chloroform.

Absorption spectra were recorded using a double-beam Perkin-Elmer Lambda 16 UV/VIS spectrophotometer. Electron microscopy was performed with a Philips CM300UT-FEG electron microscope operating at 300 kV. Emission and excitation spectra were recorded with a SPEX Fluorolog spectrofluorometer equipped with two double-grating 0.22-m SPEX 1680 monochromators and a 450-W Xenon lamp as excitation source. The emission was detected with a cooled Hamamatsu R928 photomultiplier.

To determine the luminescence quantum efficiency of a sample, the integrated emission intensity was compared to that of a reference solution with known quantum efficiency, i.e. sulphorhodamine 101 in ethanol with 90% quantum efficiency. If necessary, the solutions were diluted to have an absorbance that is in the regime where the emission intensity scales linearly with the number of absorbed photons. For single-particle luminescence measurements, small droplets of a strongly diluted QD stock solution were deposited, spread out, and dried on cover glass slides. The final density was approximately 0.1 dot/μm^2. The slides were prepared, mounted, and sealed in a flow chamber in nitrogen. Before and during the experiments, nitrogen or air was flushed through the flow chamber.

Fast spectral imaging of single dots was performed employing a confocal laser-scanning microscope (CLSM, Nikon PCM2000). The 468-nm line of an Ar-Kr CW laser was used for excitation (power $\approx$ 20 kW/cm^2). The detection channels of the microscope were coupled by optical fibers to the detectors. One of the two standard detectors was replaced by a home-built spectrograph [24,25]. In the spectrograph the light was dispersed by a prism and detected with a Peltier-cooled, back-illuminated CCD camera (NTE/CCD-1340, Princeton Instruments). The spectral resolution varied from 1–7 nm, in the wavelength range 450–750 nm. In the measurements presented, here the emission was collected using a 60×/

1.4 oil immersion objective (PlanApo, Nikon). The photomultiplier of the CLSM was first used to locate a single QD, applying a 590/60 bandpass filter (center transmission wavelength is at 590 nm, full width at half maximum [FWHM] of the band is 60 nm). The laser beam was parked at the position of single QDs, and spectra were recorded with a 6-ms dwell time. The luminescence of QDs was followed until the luminescence had been bleached away. Data are corrected for the background signal from the system and sample by subtracting the average spectrum from the time interval of the recording where the QD is not emitting. Data are further corrected for the detection sensitivity of the setup using a calibrated tungsten bandlamp [24,25]. The spectra are fitted by a Lorentzian peak function [2] for quantification of the integrated intensity, the peak position, and the peak width.

RESULTS AND DISCUSSION

High-resolution transmission electron microscopy (HR-TEM), UV-VIS absorption spectroscopy, and luminescence spectroscopy were performed to obtain information about the particle size distribution, absorption characteristics, and luminescence quantum efficiency of the CdSe/ZnS samples.

A typical absorption spectrum of a sample of CdSe/ZnS QDs is shown in Fig. 1. Because of quantum size effects, the absorption spectra of the CdSe/ZnS nanoparticles has shifted to the blue compared to the absorption spectrum of bulk CdSe (absorption onset around 730 nm [26]). The structure in the absorption band is a result of the formation of discrete energy levels caused by quantum size effects. The insert in Fig. 1 shows a histogram of the size distribution of batch 1 obtained from HR-TEM pictures. It was not possible to distinguish between the CdSe core and the ZnS shell on the HR-TEM pictures. For the histogram the size of 147 QDs was determined. The size distribution of batch 1 is about 50%. The average particle diameter of the CdSe/ZnS core shell QDs is about 3.7 nm. For batch 2, similar results were obtained.

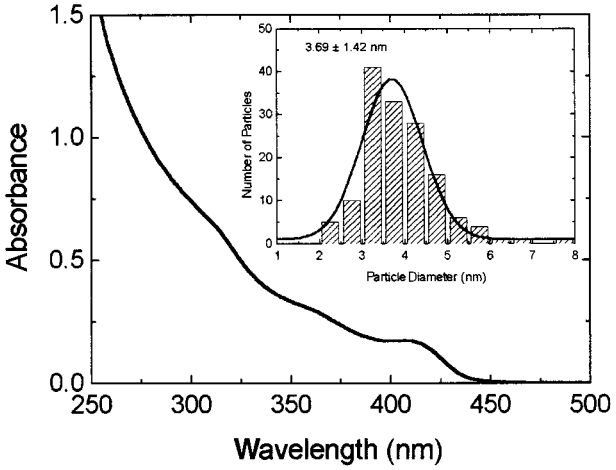

Fig. 1. UV-VIS absorption spectrum of CdSe QDs overgrown with four monolayers of ZnS (batch 1), as determined from HR-TEM photographs. The insert shows a histogram of the particle size distribution, revealing a ~50% polydispersity.

In Fig. 2a an emission and excitation spectrum of nanocrystalline CdSe with four monolayers of ZnS is shown. In addition, the emission spectrum of bare CdSe nanoparticles before the ZnS shell was grown around the CdSe core is depicted in this figure. Both emission spectra are measured under the same experimental conditions, which allows for comparison. The emission spectrum of nanocrystalline CdSe/ZnS shows a broad band centered on 650 nm. The first excitation maximum of this emission is situated around 420 nm. The red emission is assigned to the exciton emission of the CdSe. As was deduced from the HR-TEM pictures, the polydispersity of the sample is quite high. As a result the emission spectrum is rather broad (FWHM ~ 200 nm).

As is clear from Fig. 2a, the luminescence intensity increases strongly upon the growth of the ZnS shell around the CdSe core. As a result of the capping with ZnS, the luminescence quantum efficiency of the nanocrystalline CdSe/ZnS is enhanced to typically 30%. Non-radiative decay at the outer surface of the core is prevented if the capping material (ZnS in this case) passivates surface states that act as non-radiative recombination centers in bare CdSe quantum dots.

By fast spectral imaging of the (CdSe)ZnS QDs with the CLSM/spectrograph and using an excitation wavelength of 468 nm (intensity ≈20 kW/cm^2), individual QDs and their emission spectra could easily be resolved. In Fig. 2b the spectra of a few of these QDs of batch 1 are shown, with emission wavelengths of 538, 562, 601, 619, and 640 nm and FWHMs 13–18 nm. The corresponding diameters are 3.5, 4.1, 5.3, 6.1, and 7.1 nm, respectively, as calculated using the relation between diameter and emission wavelength [5]. The integrated emission spectrum over the many imaged areas (ensemble) is shown for comparison. The value of the line width is in agreement with the homogeneous broadening at room temperature by phonon dephasing processes [27]. As a result of quantum confinement effects, every single QD has its own characteristic emission wavelength, which is determined by the size of the QD. Because of the large size distribution the emission spectrum of an ensemble of CdSe/ZnS QDs is extensively broadened compared to the emission spectrum of a single QD.

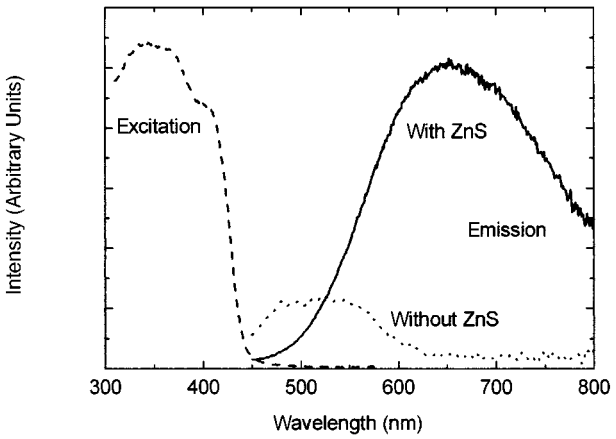

(a)

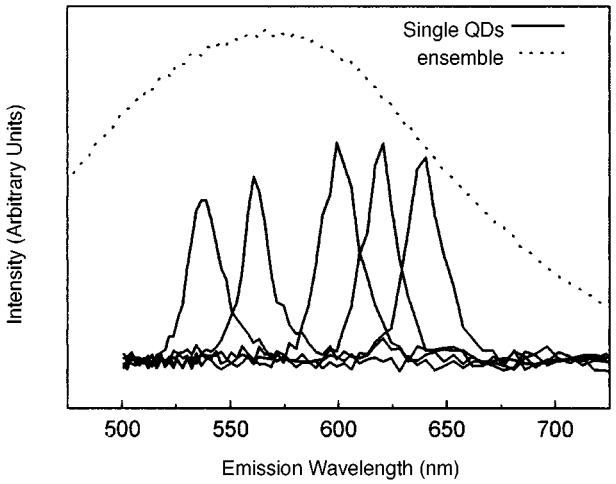

(b)

Fig. 2. (a) Fluorescence emission spectra measured at 420-nm excitation of an ensemble of QDs before (dotted line) and after (solid line) coating with four monolayers of ZnS, and the excitation spectrum. (b) Spectra of several single QDs recorded with the CLSM/spectrograph setup, compared to the spectrum of an ensemble of QDs. The emission wavelengths of the single QDs are 538, 562, 601, 619, and 640 nm (excitation wavelength 468 nm).

Luminescence spectra of individual CdSe/ZnS QDs were measured for a large number of QDs. Clear differences are observed between the time evolutions of the emission spectra of the QDs, even for dots of the same batch in the same atmosphere. To obtain reliable information on the influence of the atmosphere and the thickness of the capping layer on the spectral diffusion and on/off behavior, the emission spectra of 41 different dots were followed in time. In Fig. 3a, a typical spectrally resolved time trace (duration 80 sec) is presented of a CdSe/ZnS QD of batch 1 in *air*. Initially this QD emits at 585 nm (for about 20 sec), and then the emission wavelength starts to shift to the blue. After a blue shift of about 40 nm the emission of the QD is fully photobleached. A blow-up of a smaller part of the time trace (not shown) shows blinking of the QD [20]. Figure 3b shows spectra of the dot collected (6 ms integration) at different times. It is clear that the two spectra recorded at the later times are blue shifted with respect to the initial wavelength. The FWHM of the peaks is about 15 nm. This line width is in agreement with the homogeneous broadening by phonon dephasing processes [27]. The result of fitting of the emission maxima is shown in Fig. 4a, where the emission wavelength of a CdSe/ZnS Qd from batch 1 in *air* is depicted as a function of time. Similar results are obtained for other QDs of batch 1 and 2 in *air*, with a blue shift of 29 $\pm$ 10 nm and 29 $\pm$ 17 nm, respectively, before the luminescence disappears. In some cases an initial fast blue shift is observed, although for most QDs a behavior similar to that depicted in Fig. 4a is observed [25]. For QDs of batch 1, the luminescence intensity decreases in time and no luminescence is observed after typically 2.5 minutes. There are large differences between quenching times for individual dots, in agreement with previously reported results [9]. Because of the increased thickness of the passivating ZnS layer for QDs from batch 2, the time scales for the blue shift and the photobleaching are significantly longer (bleaching occurs on average after 3.5 minutes).

The time-evolution of the emission wavelength for a single CdSe/Zns QD of batch 1 in *nitrogen* atmosphere is depicted in Fig. 4b. Clearly, no blue shift is observed. The emission wavelength of this QD varies around an average value of about 570 nm (Fig. 4b). A spectral variation of about 10 nm is observed. This is in agreement with previous measurements, which show that over longer time periods random spectral diffusion can result in shifts of up to 10 nm [28,29]. *Contrary* to the situation in *air*, there is only random spectral diffusion in time and no shift to shorter wavelengths is observed. The time periods for which the dots show emission (until photobleaching occurs) are significantly longer for the QDs in *nitrogen* than in *air* (about 10 minutes on average for both batches).

The observed differences between the time evolution of the emission spectra of single quantum dots in *air* and in *nitrogen* provide convincing evidence that the observed blue shift of the emission in *air* is due to photo-oxidation of CdSe. From the blue shift and the well-known relation between bandgap and the diameter of CdSe particles [2,5–7], it can be calculated that the effective CdSe core diameter decreases from about 5 nm to about 4 nm before the dot is completely bleached. A change in particle diameter

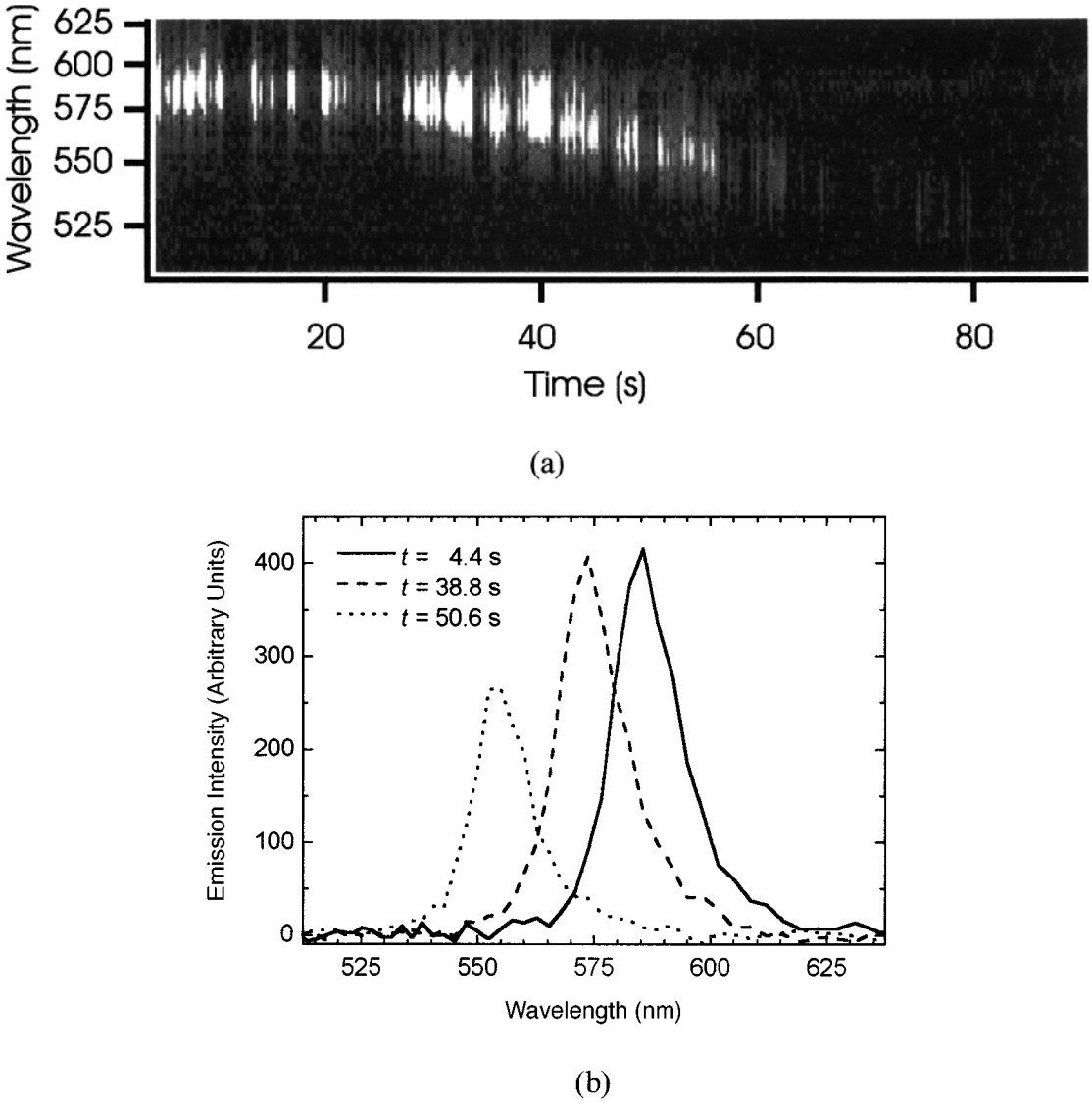

Fig. 3. Spectrally resolved time trace (a) of a CdSe/ZnS QD of batch 1 in ambient air present in the detection volume of the CLSM/spectrograph (excitation at 468 nm, room temperature). Note that the intensity is a stretched gray-scale representation. Emission spectra at different illumination times are shown in (b).

of 1 nm corresponds to photo-oxidation of almost two layers of CdSe from the surface [9]. Oxidation of CdSe nanocrystals is well known. Even under ambient conditions (without intense excitation), surface oxidation of CdSe nanoparticles has been reported [30]. The main oxidation product was suggested to be SeO_2. In the case of CdS, illumination of CdS nanocrystals leads to the photo-oxidation products Cd^{2+} and SO_4^{2-} [31–33]. For photo-oxidation of CdSe evidence for the formation of $CdSeO_x$ (x = 2, 3) has been found [5,30,31]. Here, we did not analyze the photo-oxidation products. For photo-oxidation to take place, oxygen has to diffuse through the passivating ZnS layer that has been grown on the CdSe nanocrystals. The observation that photo-oxidation occurs, indicates that the ZnS layer is not a closed epitaxial layer, but rather a layer with grain boundaries, presumably at places where ZnS islands, which started to grow at different locations on the CdSe nanocrystal, meet. At these boundaries, oxygen can diffuse to the CdSe core inside the ZnS shell. For the thicker shell (batch 2) the oxidation rate is reduced as a result of the slower diffusion of oxygen to the CdSe core through a thicker ZnS shell.

As a result of the photo-oxidation at the CdSe surface, quenching states are expected to be formed at the

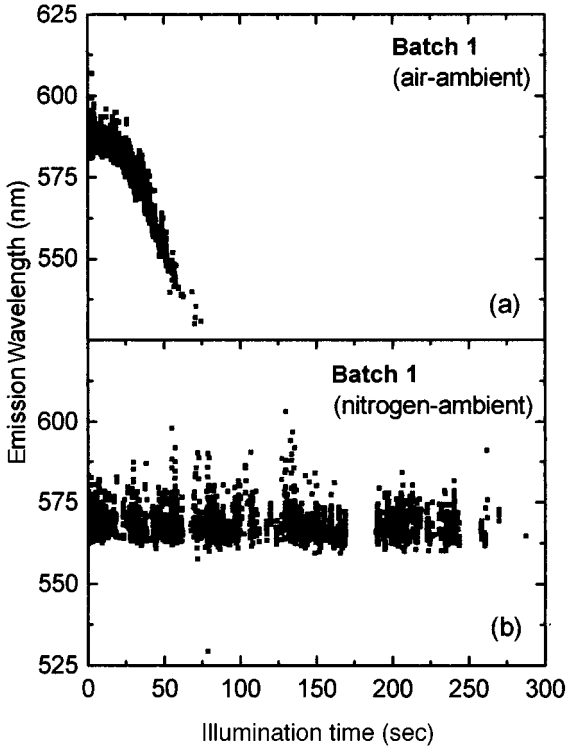

Fig. 4. Emission wavelength as a function of time of the CdSe/ZnS QD of Fig. 3, that is, batch 1 in air (a) and of a CdSe/ZnS QD of batch 1 in a nitrogen atmosphere (b).

$CdSe/CdSeO_x$ interface. The formation of surface quenching states causes a decrease of the number of photons emitted. In the single QD emission spectra a gradual decrease in light output is indeed observed as the emission shifts to shorter wavelengths. Finally, the luminescence disappears and the QD has bleached. The occurrence of photo-oxidation for QDs can explain the shorter bleaching times observed for QDs in *air*. Also, in a *nitrogen* atmosphere, photobleaching occurs, albeit after much longer times. In view of the high laser power (20 kW/cm^2), photobleaching is not unexpected. Few materials are stable against photodegradation under the presently used laser power. The nature of the photoinduced quenching states is not clear. The efficiency of the photoinduced formation of quenching states in *nitrogen* is much lower than for photo-oxidation observed in *air*. Possibly, a high-energy bi-exciton state in a single dot has enough energy to rearrange or break bonds at the CdSe/ZnS interface, which gives rise to non-radiative recombination channels and finally leads to bleaching.

The blinking behavior of the ZnS coated CdSe QDs is evident from Fig. 3. It was quantified by determining the "off" and "on" time distributions from the spectral time traces. The emission intensity was used as a means to distinguish between the "on" and "off" states. A threshold set just above the background was determined to discriminate between the "on" and "off" states. Figure 5 shows the "off" time distribution for a single QD of batch 2 in *air*.

Blinking behavior of ZnS coated CdSe QDs has been studied in detail by Kuno *et al.* [16]. Evidence was provided for an inverse power law behavior of the off-time intervals, i.e. $P(t_{off}) \propto t_{off}^{-(1+\alpha)}$. A good agreement between the experimentally observed off-time distribution over nine decades in probability density and five decades in time was observed, with $(1 + \alpha) = 1.6 \pm 0.2$. Because the process that leads to the off state is assigned to photoionization (by an Auger process) of the QD, the off-time intervals are related to recombination of the ejected charge carrier with the ionized dot. As a result the off-time interval distribution is expected to be excitation intensity independent, which has indeed been observed [16]. The most probable explanation for the inverse power law behavior is a distribution of tunneling rates for recombination processes.

Analysis of the distribution of off-time intervals for all our QDs shows that the probability density of off-time intervals can indeed be described by an inverse power law. Fitting the data in Fig. 5 to a power law distribution yields $(1 + \alpha) = 1.45$. For our QDs, we find an average value of $(1 + \alpha) = 1.4 \pm 0.2$, close to the value found by Kuno *et al.* [16] and to earlier work by our group [34]. This value is the average of an analysis for 41 QDs, both in air and in nitrogen atmosphere. Because of the limited statistics, a significant difference between the values for $(1 + \alpha)$ in air and nitrogen has not been observed. A difference is expected because the shrinking of the CdSe core and the formation of a $CdSeO_x$

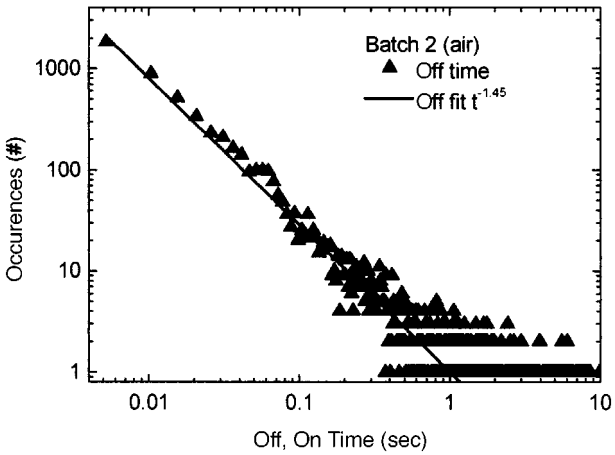

Fig. 5. Off-time distribution for a QD of batch 2 in air. The off-time distribution of this particular QD can be fitted with $(1 + \alpha) = 1.45$.

at the interface is likely to influence the tunneling rate for recombination of an ejected charge carrier and an ionized dot. Further research is in progress on the differences in the blinking of QDs in air and nitrogen.

The potential application of single QDs as luminescent labels (e.g., in biological systems) is based on the high stability in combination with a relative narrow emission band and a large Stokes' shift [10,11]. The total number of photons emitted by a single QD until bleaching occurs is an important number. For single dye molecules (e.g., Rhodamine [35–37]) the highest number of photons emitted before bleaching is around 10^6 at room temperature. Based on an overall efficiency of about 5% for the system (i.e., 1 out of every 20 emitted photons is counted), the number of photons emitted by a single QD before bleaching occurs, is typically 2×10^7, with numbers exceeding 10^8 for the more robust QDs. These numbers are more than an order of magnitude higher than for single dye molecules, which reflects the higher stability of inorganic chromophores such as semiconductor QDs.

Surprisingly, the total number of photons emitted before bleaching occurs is not much less for QDs in air than for QDs in nitrogen. The shorter lifetime of QDs in air is compensated for by a higher initial photon count in air. The initial emission intensity is about two times higher for QDs in air (about 3,000 counts in air versus 1,500 counts in nitrogen during the 6-ms integration period for the highest QDs). At present, further experiments are conducted to provide more precise information on the difference in initial light output. A possible explanation for the higher initial light output in air is quenching of QD defect luminescence by oxygen. It is well known that in addition to the fast (nanosecond) exception emission, also relatively long-lived (microsecond) defect omission can occur in QDs [31,38]. Because of the long lifetime, the fast photon absorption and emission process is interrupted, until the long-lived excited state has returned (via radiative or non-radiative relaxation) to the ground state. If oxygen can quench the defect luminescence, a higher exception emission yield is expected by reduction of the time spent in the "dark state." For CdSe, we have not found studies on the role of oxygen on the efficiency of the defect emission. For other II–VI semiconductors such as Cds and ZnS, it has been established that oxygen can quench the defect-related emission [31,38]. If the same occurs for CdSe QDs, this can explain the higher initial light output observed for CdSe QDs in air. The presently applied excitation power (20 kW/cm^2) yields initial intensities of 1,000–3,000 counts in 6 ms. Assuming a 5% collection efficiency, this corresponds to time intervals of 100–300 ns between emission of photons. In this situation, relaxation to a trap state with a microsecond lifetime will reduce the number of photons emitted and a fast return to the ground state by non-radiative relaxation enhances the photon output. A similar situation has been reported for dye molecules where higher fluorescence light yields were measured by quenching of the triplet state luminescence [39].

CONCLUSION

In this paper, we have presented time-resolved luminescence measurements on single CdSe/Zns core-shell QDs. A clear blue shift in the emission wavelength of on average 30 nm is observed for QDs in ambient air. In contrast, this shift is not observed for QDs in a nitrogen atmosphere. Moreover, the bleaching time and initial emission intensity of single QDs are influenced by the presence of oxygen. The results are explained by photoinduced oxidation of the CdSe crystallites.

ACKNOWLEDGMENTS

We gratefully acknowledge the Netherlands Technology Foundation (STW) and the Netherlands Council for Earth and Life Sciences (ALW) of the Netherlands Organization for Scientific Research (NWO) for financial support.

REFERENCES

1. A. P. Alivisatos (1996) *J. Phys. Chem.* **100**, 13226–13239.
2. S. V. Gaponenko (1998) *Optical Properties of Semiconductor Nanocrystals*, Cambridge University Press, Cambridge, U. K.
3. Al. L. Efros and M. Rosen (2000) *Annu. Rev. Mater. Sci.* **30**, 475–521.
4. A. D. Yoffe (2001) *Adv. Phys.* **50**, 1–208.
5. B. O. Dabbouosi, J. Rodriguez-Viejo, F. V. Mikulec, J. R. Heine, H. Mattoussi, R. Ober, K. F. Jensen, and M. G. Bawendi (1997) *J. Phys. Chem. B* **101**, 9463–9475.
6. S. Empedocles and M. G. Bawendi (1996) *Acc. Chem. Res.* **32**, 389–396.
7. F. V. Mikulec, M. Kuno, M. Bennati, D. A. Hall, R. G. Griffin, and M. G. Bawendi (2000) *J. Am. Chem. Soc.* **122**, 2532–2540.
8. S. A. Blanton, A. Dehestani, P. C. Lin, and P. Guyot-Sionnest (1994) *Chem. Phys. Lett.* **229**, 317–322.
9. M. Nirmal, B. O. Dabbousi, M. Bawendi, J. J. Macklin, J. K. Trautmann, T. D. Harris, and L. E. Brus (1996) *Nature* **383**, 802–804.
10. M. Bruchez, Jr., M. Moronne, P. Gin, S. Weiss, and A. P. Alivisatos (1998) *Science* **281**, 2013–2016.
11. W. C. W. Chan and S. Nie (1998) *Science* **281**, 2016–2018.
12. M. Dahan, T. Laurence, F. Pinaud, D. S. Chemla, A. P. Alivisatos, M. Sauer, and S. Weiss (2001) *Opt. Lett.* **26**, 825–827.
13. D. Gerion, F. Pinaud, S. C. Williams, W. J. Parak, D. Zanchet, S. Weiss, and A. P. Alivisatos (2001) *J. Phys. Chem B* **105**, 8861–8871.

14. Al. L. Efros and M. Rosen (1997) *Phys. Rev. Lett.* **78**, 1110–1113.
15. U. Banin, M. Bruchez, A. P. Alivisatos, T. Ha, S. Weiss, and D. S. Chemla (1999) *J. Chem. Phys.* **110**, 1195–1201.
16. M. Kuno, D. P. Fromm, H. F. Hamann, A. Gallagher, and D. J. Nesbitt (2000) *J. Chem. Phys.* **112**, 3117–3120.
17. R. G. Neuhauser, K. T. Shimizu, W. K. Woo, S. A. Empedocles, and M. G. Bawendi (2000) *Phys. Rev. Lett.* **85**, 3301–3304.
18. S. A Empedocles and M. G. Bawendi (1997) *Science* **278**, 2114–2117.
19. S. R. Cordero, P. J. Carson, R. A. Estabrook, G. F. Strouse, and S. K. Buratto (2000) *J. Phys. Chem B* **104**, 12137–12142.
20. W. G. J. H. M. Van Sark, P. L. T. M. Frederix, D. J. Van den Heuvel, H. C. Gerritsen, A. A. Bol, J. N. J. Van Lingen, C. De Mello Donegá, and A. Meijerink (2001) *J. Phys. Chem. B* **105**, 8281–8284.
21. M. A. Hines and P. Guyot-Sionnest (1996) *J. Phys. Chem.* **100**, 468–471.
22. W. G. J. H. M. Van Sark, P. L. T. M. Frederix, A. A. Bol, D. J. Van den Heuvel, H. C. Gerritsen, and A. Meijerink (2002) *Phys. Chem. Chem. Phys.*, submitted for publication.
23. A. A. Bol (2001) Ph.D. Thesis, Utrecht University.
24. P. L. T. M. Frederix, M. A. H. Asselbergs, W. G. J. H. M. Van Sark, D. J. Van den Heuvel, W. Hamelink, E. L. De Beer, and H. C. Gerritsen (2001) *Appl. Spec.* **55**, 1005–1012.
25. P. L. T. M. Frederix (2001) Ph.D. Thesis, Utrecht University.
26. W. M. Yen and S. Shionoya (1999) *Phosphor. Handbook*, CRC Press, Boca Raton, FL, p. 233.
27. X.-Q. Li and Y. Arakawa (1999) *Phys. Rev. B* **60**, 1915–1920.
28. S. A. Blanton, M. A. Hines, and P. Guyot-Sionnest (1996) *Appl. Phys. Lett.* **69**, 3905–3907.
29. S. A. Empedocles, R. Neuhauser, K. Shimizu, and M. G. Bawendi (1999) *Adv. Mater.* **11**, 1243–1256.
30. J. E. Bowen Katari, V. L. Colvin, and A. P. Alivisatos (1994) *J. Phys. Chem.* **98**, 4109–4117.
31. A. Henglein (1988) *Top. Curr. Chem.* **143**, 113–180.
32. D. E. Dunstan, A. Hagfeldt, M. Almgren, H. O. G. Siegbahn, and E. Mukhtar (1990) *J. Phys. Chem.* **94**, 6797–6804.
33. L. Spanhel, M. Haase, H. Weller, and A. Henglein (1987) *J. Am. Chem. Soc.* **109**, 5649–5655.
34. W. G. J. H. M. Van Sark, P. L. T. M. Frederix, D. J. Van den Heuvel, M. A. H. Asselbergs, I. Senf, and H. C. Gerritsen (2000) *Single Mol.* **1**, 291–298.
35. I. Rosenthal (1978) *Opt. Comm.* **24**, 164–166.
36. A. L. Huston and C. T. Reimann (1991) *Chem. Phys.* **149**, 401–407.
37. T. Schmidt, G. J. Schütz, W. Baumgartner, H. J. Gruber, and H. Schindler (1996) *Proc. Natl. Acad. Sci. USA* **93**, 2926–2929.
38. N. Chestnoy, T. D. Harris, R. Hull, and L. E. Brus (1986) *J. Phys. Chem.* **90**, 3393–3399.
39. L. Song, C. A. G. O. Varma, J. W. Verhoeven, and H. J. Tanke (1996) *Biophys. J.* **70**, 2959–2968.